Plasmonics (2012) 7:279–286
DOI 10.1007/s11468-011-9304-6

# Laser-Driven Precipitation and Modification of Silver Nanoparticles in Soda Lime Glass Matrix Monitored by On-line Extinction Measurements

**Michał Grabiec · Aleksandra Wolak · Olivier Véron · Jean-Philippe Blondeau · Nadia Pellerin · Mathieu Allix · Stephane Pellerin · Krzysztof Dzierżęga**

Received: 25 January 2011 / Accepted: 20 November 2011 / Published online: 13 December 2011

**Abstract** In this work, we investigated the effect of nanosecond laser irradiation at 532 nm on precipitation of Ag nanoparticles (NPs) in soda lime glasses doped with silver in the $Ag^+$–$Na^+$ ion-exchange process. Formation and subsequent modification of Ag NPs during laser irradiation were studied by on-line extinction measurements making use of the localized surface plasmon resonance (LSPR). These investigations were further completed using scanning and transmission electron microscopies to examine the average size and distribution of nanoparticles within the sample. It has been shown that formation of NPs, its kinetics and the particle size strongly depend on the fluence and the total number of deposited laser pulses. It has been found that Ag NPs form after some specific number of pulses and they rapidly grow in size and number until some maximal value of extinction has been reached. Further irradiation of such samples only results in destruction of precipitated NPs due to photobreakup, laser ablation confirmed by strong plasma emission observation. Moreover, due to strong irradiation, the host matrix can also be affected by changing its refractive index which manifests as the blue shift of the LSPR.

**Keywords** Surface plasmon resonance (SPR) · Metal nanoparticles · Laser induced plasma · Composite nanomaterials · Ion exchange

## Introduction

Large interest in metal nanoparticles (MNPs) and their composites is dictated by their potential technological and biomedical applications such as optical elements [1–3], sub-wavelength optical devices [4, 5], optical data storage [6] or chemical and biological sensing and labeling [7, 8]. These applications are based on specific optical properties of MNPs that differ drastically from those of bulk metals. The unique optical properties of such noble MNPs as silver, gold or copper are dominated by coherent oscillations of conduction-band electrons in response to the electric field of the electromagnetic radiation of light. This resonant excitation is known as localized surface plasmon resonance (LSPR) which appears in the UV/visible spectral range. The LSPR characteristics like amplitude or spectral location and bandwidth strongly depend on the nanoparticle size, shape, as well as on its local environment [9].

Ion-exchange technique [10, 11] combined with electron beam irradiation [12], thermal annealing [13, 14]

---

M. Grabiec (✉) · A. Wolak · K. Dzierżęga
Marian Smoluchowski Institute of Physics,
Jagiellonian University, ul. Reymonta 4,
30-059 Kraków, Poland
e-mail: michal.grabiec@uj.edu.pl

O. Veron · J-P. Blondeau
PRISME Institute EA 4229, Université d'Orleans,
21 Rue Loigny La Bataille, 28000 Chartres, France

N. Pellerin · M. Allix
CEMHTI, CNRS/Université d'Orléans,
Avenue de la Recherche Scientifique,
45071 Orléans cedex 2, France

S. Pellerin
GREMI-Site de Bourges, Université d'Orléans/CNRS,
Rue Gaston Berger, BP4043 18028 Bourges cedex, France

or laser irradiation [15, 16] provides simple method for MNP synthesis in glasses. After inclusion of metal ions into the glass matrix in the process of ion-exchange with alkaline ions of glass, the formation of MNPs involves reduction of metal ions followed by diffusion and aggregation of metal atoms [17].

A relatively new approach of producing MNPs in glass involves laser irradiation. Contrary to most of methods, except electron beam, laser irradiation can be space selective, so the growth of MNPs can be locally photoactivated. Reduction of metal ions and aggregation of atoms have been achieved using cw sources [18, 19] or nano- [20] and femtosecond [21] laser pulses of UV and visible wavelengths. The effect of irradiation strongly depends on pulse duration, laser fluence and radiation wavelength. In the case of femtosecond lasers, high-intensity pulses can induce non-bridging oxygen hole centres, E’ centres (hole and electron pairs), as well as they can cause photo-ionization of metal ions such as $Ce^{3+}$, $Sb^{2+}$ or $Fe^{2+}$ [22]. Besides of trapping of electrons and holes by sites to form colour centres, some electrons are trapped by metal cations which leads to formation of neutral metal atoms. However, for ultrashort laser pulses, since the heat transfer from electrons to the glass matrix is very limited, diffusion and subsequent aggregation of silver atoms need either additional annealing [23, 24] or laser pulses of high fluence [21, 25]. Similarly, in the case of nanosecond laser radiation, both reduction of cations and aggregation of metal atoms can be achieved during single pulse provided its intensity is high enough to create free electrons and holes [26].

Although all of these processes have been extensively studied, the complete mechanism of the growth of metal NPs in glass by laser irradiation is not yet fully recognized. In great part, this is due to the lack of methods enabling to characterize the composite samples during precipitation of NPs. Thus, on-line extinction measurements would bring a lot of information about these processes, for instance on the kinetics of NP growth as it was inferred from ex situ measurements by De Marchi et al. [27].

In this paper, we investigate the precipitation of Ag NPs in soda lime glass (containing silver ions) as the result of irradiation by nanosecond laser pulses at 532 nm. The optical characteristics such as the extinction and plasma emission spectra were measured during laser irradiation of the glass samples, i.e. in real-time of the NP precipitation process. The standard optical microscopy, photometry and electron microscopy (scanning (SEM) and transmission (TEM)) were used to investigate the samples after irradiation.

## Experimental

In our experiments, we used commercial soda lime glass slides ($76 \times 76 \times 1$ $mm^3$) with composition (percent mole) of 72.2 $SiO_2$, 1.2 $Al_2O_3$, 14.3 $Na_2O$, 1.2 $K_2O$, 6.4 CaO, 4.3 MgO, 0.03 $Fe_2O_3$ and 0.3 $SO_3$. The ion-exchanged (I-E) samples were obtained by immersing for 10 min the glass slides in a molten salt bath of $NaNO_3-AgNO_3$ (10%mol) at temperature of 320°C. During immersion, part of sodium ions at glass surface is replaced by silver cations from the solution, and Ag–O bonds are formed to a depth of about 6 μm below the surface. The thickness of the layer with Ag ions was estimated using SEM patterns in the back scattering mode [26]. Due to high extinction of glass layers containing MNPs, in order to eliminate the interference effects between two surfaces during optical measurements, one of these surfaces was polished to remove the ion-exchanged layer.

The experimental setup used to study precipitation of Ag NPs is shown in Fig. 1. The I-E glasses were irradiated by the second harmonic ($\lambda_L = 532$ nm, $E_L = 2.33$ eV) of the pulsed Nd:YAG laser. The laser delivered pulses of 6 ns duration (full width at half maximum) at the 10-Hz repetition rate, with maximum pulse energy of 130 mJ and of approximately gaussian cross-sectional area. The laser beam was focused to the spot of about 3.6 mm diameter onto the sample surface using 45 cm focal length lens. The maximal fluence ($F_L$) of the single laser pulse was about 1.4 $J/cm^2$, and it was attenuated using a polarizer and a half-wave plate.

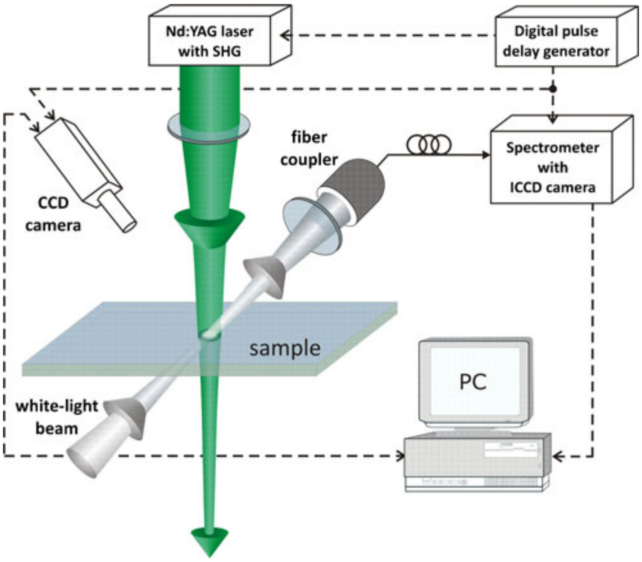

**Fig. 1** Experimental setup for irradiation of the I-E glass samples and for on-line extinction and plasma emission measurements

The laser irradiated area of the sample was simultaneously illuminated by a collimated white light beam from a halogen lamp with the spot diameter of about 2 mm. The light transmitted through the sample was coupled into a fibre and then to the spectrometer equipped with an image intensified charge-coupled device (ICCD) camera. The extinction measurements of the glass samples were performed for the spectral range between 380 and 490 nm with resolution of 0.82 nm. The measurements were carried out 100 μs after each laser pulse with 26 ms integration time. Such timing, controlled by digital delay pulse generator, ensured that neither luminescence from Ag NPs nor plasma emitted light was collected. In order to avoid saturation of the ICCD, a glass-coloured filter was placed in the path of the white light beam to attenuate the intensity of the red part of the spectrum of the halogen lamp.

The system of the fibre coupler and the spectrometer with the ICCD camera was also used to investigate plasma emission during laser irradiation. Emitted light was acquired for 100 μs starting 1 μs after each pulse to avoid collection of strong continuous plasma radiation. During laser irradiation, the surface of the sample as well as total plasma emissivity and its spatial distribution were monitored by another CCD camera synchronized to the Nd:YAG laser. Additional, more precise measurements of the extinction of the central part (1 mm diameter) of the irradiated samples were performed ex situ using commercial spectrophotometer (SHIMADZU 1200 PC). The measurements were carried out in the 320–850-nm spectral range with the resolution of 1 nm. Besides optical measurements, the samples with precipitated silver nanoparticles were investigated by SEM coupled with EDX analysis and TEM to verify the size of Ag NPs and their spatial distribution within the sample. Samples for transmission electron microscopy were prepared by gently scratching the sample surface. The powder we obtained was then crushed, diluted in ethanol, and deposited onto a holey carbon film, supported by a copper grid. Bright field imaging and electron diffraction studies were carried out with a Philips CM20 electron microscope operating at 200 kV. Finally, profilometric measurements were performed with DEKTAK 150, VEECO device.

## Results and Discussion

The extinction measurements were performed for the glass samples before and after ion-exchange process to examine the presence of the LSPR and thereby formation of silver nanoparticles, and the results are presented in Fig. 2. As one could expect, no LSPR was detected for pure glass and ion-exchanged samples, although small increase of extinction was observed in the latter case. This effect is due to $Ag^+$ implemented in the silica matrix which can form colour centres [6], whereas most of irradiated I-E samples reveal considerable increase of their extinction. This increase is the effect of laser scattering from the surface of the modified glass sample but predominantly it is due to the LSPR of Ag NPs which is located near 440 nm. The extinction of the irradiated I-E glasses manifests strong dependence on the number and the fluence of deposited laser pulses. Figure 3 presents extinction of the ion-exchanged samples after irradiation by different number of laser pulses with the fluence of 1.35 J/cm$^2$. After applying 25 pulses, the extinction increases at all wavelengths and the LSPR peak is already well pronounced. This peak is further enhanced until 50 pulses are deposited and subsequent irradiation makes the LSPR contribution only to diminish.

Variations in extinction directly influence the colour of the samples as it is shown in insets of Fig. 3. First, for low number of pulses, only the central part becomes yellowish and the colored area expands with the number of pulses. When the magnitude of the LSPR is maximal (after 50 pulses), the whole irradiated area of the sample gets dark yellow with well-defined brown ring at the border of the laser beam, while continuing irradiation the colour of the central part of the irradiated area gets less and less intense and finally becomes transparent with the border still dark brown.

Such extinction variations can be explained by formation and modification of silver nanoparticles which are responsible for the LSPR and their presence was confirmed by TEM measurements (see Fig. 4). In

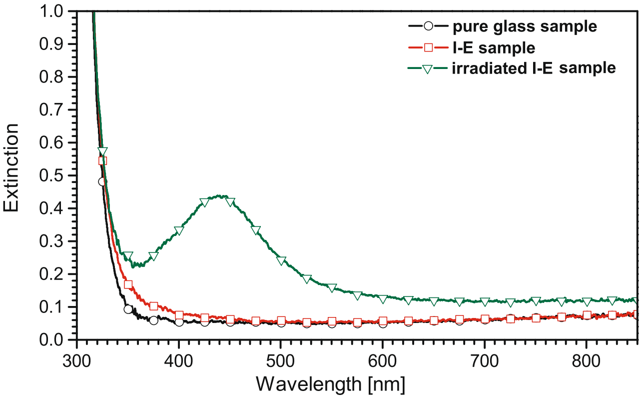

**Fig. 2** Extinction spectra of glass samples before and after ion-exchange as well as after laser irradiation by 50 laser pulses with $F_L$ =1.35 J/cm$^2$

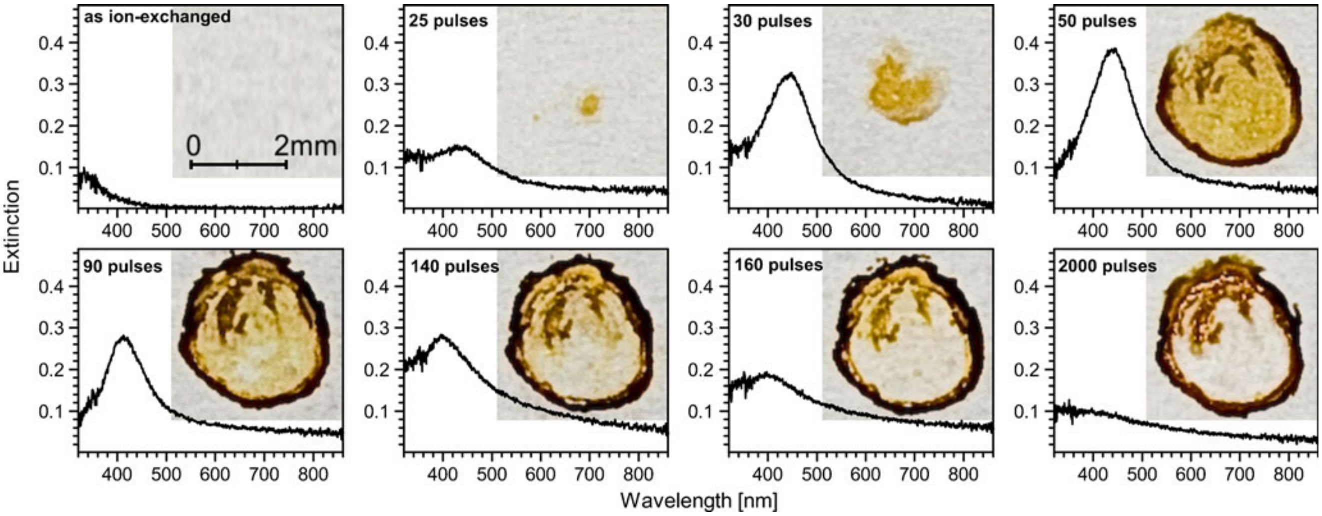

**Fig. 3** Extinction spectra and corresponding images (in *insets*) of the I-E glass samples after irradiation by the specific number of pulses with fluence of 1.35 J/cm$^2$

this figure, the selected grain shows numerous silver nanoparticles (in black) in the glass matrix. Their size is in the 5–10-nm range with larger NPs also observed. Electron diffraction confirms the crystalline nature of the silver particles and their nanometric scale. A careful analysis of the pattern allows the identification of four $d_{\mathrm{hkl}}$ reflections observed at 2.36 Å, 2.04 Å, 1.44 Å and 1.23 Å which correspond to the expected 111, 002, 022 and 311 indexation planes of the Ag metallic structure (crystallizing in the FM-3M space group with $a$ = 4.085 Å), respectively. The observed nanostructures can be undoubtedly identified as metallic silver NPs.

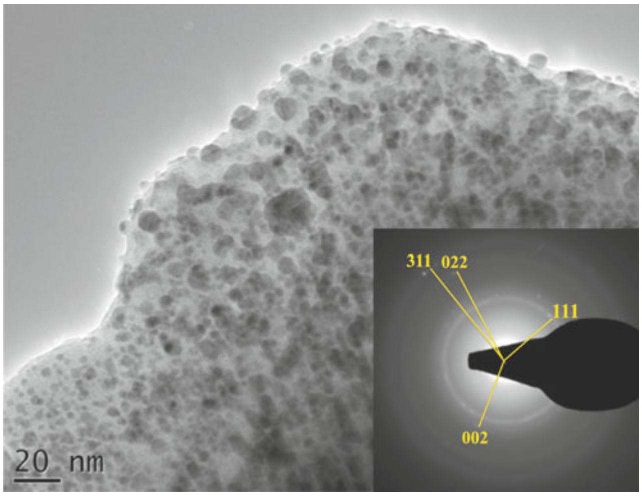

**Fig. 4** Bright field TEM image of Ag nanoparticles observed in the I-E glass after irradiation by 160 laser pulses with the fluence of 1.35 J/cm$^2$. The corresponding electron diffraction pattern is embedded

The LSPR resonance was clearly observed only after irradiation by a specific number (from 25 to 160) of laser pulses. For 25 laser pulses, the maximum of the LSPR occurs at 440 nm. After 30 pulses, the magnitude of the LSPR is even higher, but its maximum is red-shifted by about 6 nm. Extra 20 pulses result in further enhancement of the LSPR which is already observed over the whole irradiated area (see insets in Fig. 3). Nevertheless, accumulation of 50 pulses leads to the formation of the brown ring around this area. This effect can be associated with ablation of the sample in the hot central parts interacting with the laser beam and condensation of silver cations and atoms in the cooler outer regions where they cluster and form nanoparticles. Such processes finally result in bleaching of the sample after next several hundreds of laser pulses since a large part of silver is removed and therefore only very weak LSPR is observed.

Figure 5 presents on-line measured extinction spectra depending on the number of deposited laser pulses with different fluences per pulse. The strong impact of the laser fluence on the LSPR and its evolution is apparent. First of all, under conditions of our experiment, no LSPR is observed using the pulses with fluence lower than about 0.3 J/cm$^2$. It is also evident that the higher the fluence, the lower is the number of pulses required to induce measurable increase of extinction. For instance, approximately 210 pulses of $F_{\mathrm{L}} = 0.54$ J/cm$^2$ are required to raise extinction by 0.1 while the same change is achieved with only 30 pulses of $F_{\mathrm{L}} = 1.35$ J/cm$^2$. Moreover, different evolution of extinction spectra is observed while irradiating the samples with pulses of low ($< 0.5$ J/cm$^2$) and high

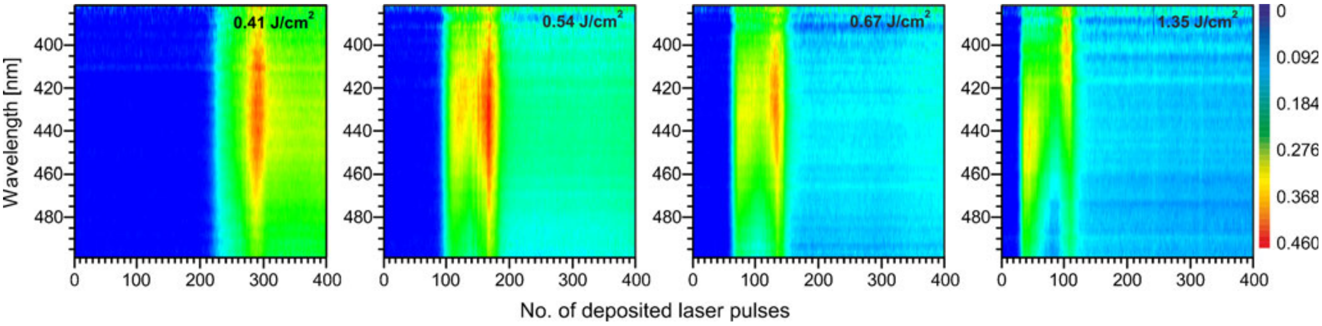

**Fig. 5** Extinction of the I-E samples as a function of the number of laser pulses and wavelength obtained for various fluences of the single pulse

fluence with abrupt change of its position in the second case. All aforementioned effects are also evident by monitoring the total extinction, i.e. integrated over the measured spectral range with substracted extinction of pure glass (see Fig. 6). Threshold number of pulses decreases with the fluence while the rate of precipitation of NPs is increasing. It is also evident that for lower fluences, extinction remains high or even increases after large number of pulses while high fluence results in sample bleaching.

According to the Mie theory, variations of the LSPR spectra result from variations of the size and the number of silver NPs contained in the glass matrix. Figure 7 shows the average radius and the concentration of Ag NPs depending on the number of deposited laser pulses and their fluence. The radius and concentration were calculated by fitting the optical spectra as it is discussed in [28, 29]. The average size of NPs is consistent with TEM results.

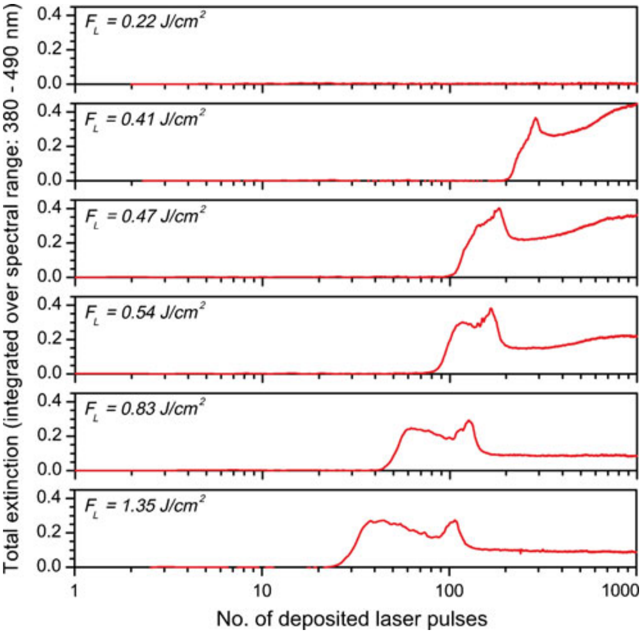

**Fig. 6** Total extinction after subtraction of extinction of the pure glass as a function of the number of laser pulses deposited onto the I-E samples

As it is shown in Fig. 7, both the concentration of Ag NPs and their size are rapidly increasing after some specific number of pulses and until the maximum value of the extinction (the first maximum, see Fig. 6) is reached. From microscopic point of view the laser-induced precipitation of Ag NPs in glass matrix can be explained by photonic and thermal processes. Since the photon energy (2.33 eV, $\lambda_L = 532$ nm) is lower than the absorption edge of the glass (3.65 eV), the multiphoton processes must play the principal role in formation of silver nanoaggregates which is confirmed by strong spatial (within the laser beam) dependence of this process [6, 24].

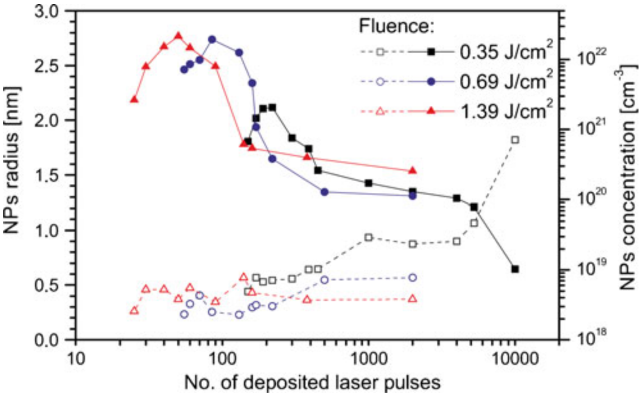

**Fig. 7** The average radius of Ag NPs (*filled symbols*) and concentration of NPs (*empty symbols*) as a function of the number of laser pulses deposited onto the I-E samples with fluences of 0.35, 0.69 and 1.35 J/cm$^2$

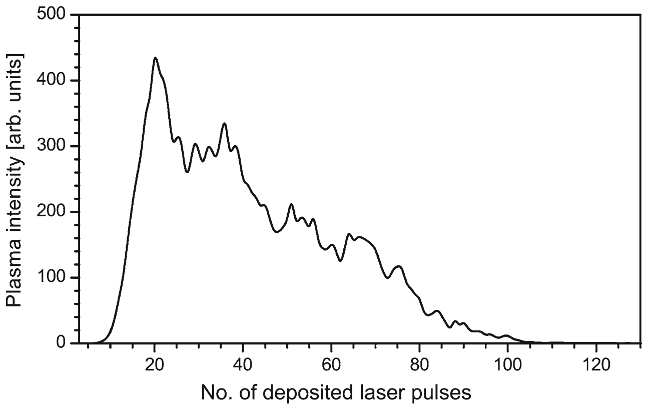

**Fig. 8** Plasma intensity (integrated over the spectral range of 380–490 nm) recorded 1 μs after laser pulse as a function of the number of laser pulses irradiating the I-E sample. The fluence of the single pulse was 1.22 J/cm$^2$

After each laser pulse, some number of nucleation centres are formed through the reduction of Ag$^+$ to Ag$^0$ atoms [18, 30]. The existence of the threshold number of laser pulses (at given fluence) above which the LSPR is observable suggests that density of nucleation centres in the central region of the laser-treated zone exceeds the threshold density. For such density, nucleation centres, Ag$^0$ and Ag$^+$ cations, are close enough to each other to agglomerate via diffusion. The laser energy, absorbed by conduction electrons of NPs, can be transferred to the glass matrix, since the pulse duration is long enough. This can cause local heating of the sample that facilitates silver diffusion. Although low repetition rate of laser pulses precludes accumulation of the heat in the irradiated area, nevertheless Ag$^+$ cations can migrate to nucleation centres during the single laser pulse, and the agglomeration of Ag atoms and cations can occur resulting in precipitation of NPs. The rate of the aggregation is enhanced after first NPs are formed, and the LSPR absorption band appears which makes laser radiation to be more and more absorbed resulting in increase of temporary temperature in the irradiated area of the sample. This, in turn, rises the diffusion rate of Ag ions and atoms so that the growth of NPs is accelerated. As the process of irradiation continues, NPs start to decrease in size and number which is caused predominantly by high absorption which results in photo-fragmentation and laser ablation [31] accompanied by plasma generation. Despite absorption of laser radiation by the I-E glass samples is relatively low, the presence of silver NPs makes it to grow significantly even at the wings of the LSPR which results in heating and vaporization of the NPs. The latter should occur when absorbed energy exceeds the latent heat of vaporization, $L_v$ of the NP. The threshold fluence, $F_{th}$, above which bulk silver evaporates can be calculated for metals from the formula [32]:

$$F_{th} = \rho \; L_v \, a^{1/2} \tau^{1/2} \,, \tag{1}$$

where $\rho$ is density of the sample, $a$ is its thermal diffusivity ($a = \kappa / \rho C_p$, $\kappa$ and $C_p$ are the thermal conductivity and the specific heat, respectively) while $\tau$ is duration of the laser pulse. For the laser wavelength of 532 nm and 6 ns pulse, $F_{th}$ is about 2.6 J/cm$^2$ for silver and is much lower than the threshold fluence for soda lime glass (<20 J/cm$^2$) [33]. Although, in this experiment, the laser fluence was below $F_{th}$, the plasma was already observed during irradiation of the I-E samples by pulses with fluences higher than only about 0.5 J/cm$^2$. The plasma intensity (from pulse to pulse) was directly related to concentration of Ag NPs (see Figs. 5 and 8). The lowering of the threshold fluence for laser ablation process can be explained by increased absorption of laser radiation due to the presence of silver NPs as compared to bulk silver.

The ablation process manifests itself by the spectral lines of Ag in the plasma spectrum (see Fig. 9). Besides

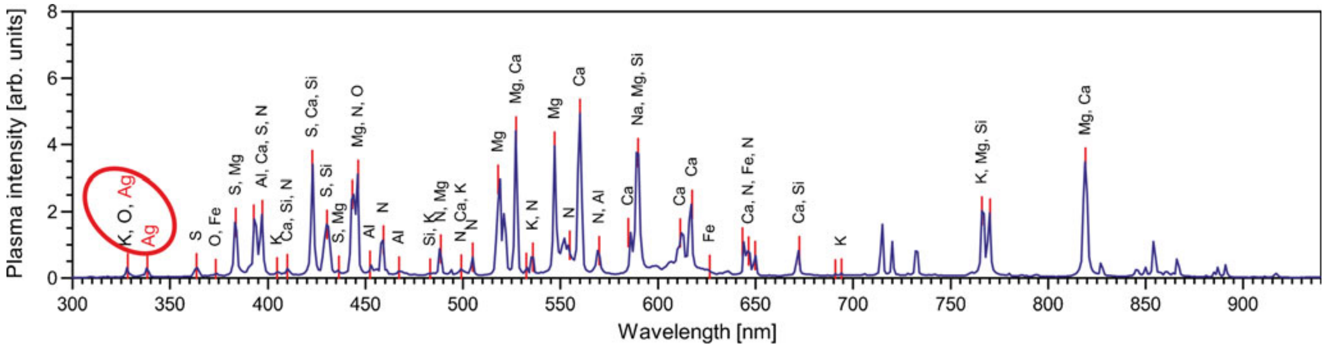

**Fig. 9** Plasma spectrum emitted after the 37th laser pulse with fluence of 1.22 J/cm$^2$

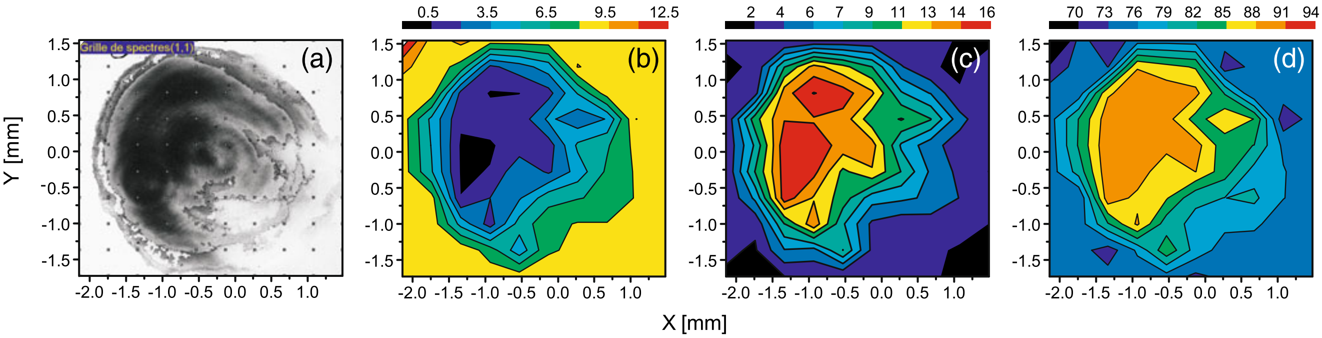

**Fig. 10** An image (**a**) and distributions of Ag (**b**), Na (**c**) and Si (**d**) relative concentrations (percent mole) obtained using SEM for the I-E sample irradiated by 1,000 laser pulses with fluence of 1.35 J/cm$^2$

NP precipitation and modification, laser radiation and plasma can strongly affect the glass matrix, promoting some thermal effects and defragmentation of NPs which results in change of its refractive index. This way we can explain large blue shift of the second maxima of the LSPR (see Fig. 5), i.e. by lowering the refractive index of the host matrix during its interaction with laser pulses. Since mutual interaction between plasma and NPs is not yet well recognized, this issue needs further investigations.

Since most processes involving interaction between laser pulse and the I-E sample like ablation or silver migration take place on or near the surface, additional SEM and EDX measurements were performed to examine the surface quality and constitution after irradiation, and the results are presented in Fig. 10. It is clear that unlike Na and Si, concentration of Ag increases moving outwards the centre of the irradiated area which corresponds to brown rings as observed in insets of Fig. 3. However, these results are strongly affected by the roughness of the surface of the irradiated zone. Poor quality of the surface was confirmed by the profilometric measurements.

## Summary and Conclusions

In this work, we have investigated the effect of nanosecond laser irradiation on precipitation of Ag nanoparticles in soda lime glasses doped with silver in the $Ag^+$–$Na^+$ ion-exchange process. The growth of Ag NPs and the rate of their modification during laser irradiation were studied by on-line extinction measurements making use of the localized surface plasmon resonance. These investigations were further completed using scanning and transmission electron microscopies as well as photometric measurements of the irradiated samples. TEM served to verify the average size of nanoparticles and their distribution while SEM and EDX was used to determine concentrations of various elements in specific regions on the surface of the samples.

It has been shown that the process of formation of NPs, its rate and the average size of NPs strongly depend on the fluence and the total number of deposited laser pulses. It has been found that Ag NPs start to form after some specific number of pulses, and they rapidly grow in size and number until some maximal value of extinction has been reached. Most likely aggregation begins when some minimal number of nucleation centres and $Ag^0$ has been created but also when their diffusion length, during the pulse, is comparable to the distance between Ag atoms. The rate of diffusion rises with temperature of the sample which is significantly increased during the laser pulse, in particular in regions with NPs as they can absorb a lot of energy from the pulse through the LSPR.

Further irradiation of the I-E samples only results in their destruction via photo-breakup, laser ablation and migration of Ag ions and atoms outside the laser irradiated area. The laser ablation was clearly indicated by plasma emission and Ag spectral lines observed in its spectrum. Moreover, the host matrix is also considerably affected, and the sudden change of its refraction manifests as the abrupt blue shift of the LSPR.

Finally, the on-line extinction measurements have proved to be the valuable method in studying the process of nanoparticles precipitation and seems to be the mean to achieve controlled metal aggregation in transparent host matrices.

**Acknowledgements** We wish to thank Nadège Ollier and Mohamed Chérif Sow from Jean Monnet University in Saint-Etienne for their profilometric measurements. The research was carried out with the equipment purchased thanks to the financial support of the European Regional Development Fund in the framework of the Polish Innovative Economy Operational Program (contract no. POIG.02.01.00-12-023/08). This work was also supported by the APR ContVerColl of the Région Centre (France) and by the Polish Ministry of Science and Higher Education grant NN202 031136.

## References

1. Vollath D (2008) Nanomaterials: an introduction to synthesis, properties and applications. Wiley-VCH, Weinheim
2. Maier SA (2007) Plasmonics: fundamentals and applications. Springer, Berlin
3. De Marchi G, Caccavale F, Gonella F, Mattei G, Mazzoldi P, Battaglin G, Quaranta A (1996) Silver nanoclusters formation in ion-exchanged waveguides by annealing in hydrogen atmosphere. Appl Phys A 63:403–407
4. Salerno JR, Krenn B, Lamprecht G, Schider H, Ditlbacher N, Felidj A, Leitner, Aussenegg F (2002) Plasmon polaritons in metal nanostructures: the opto-electronic route to nanotechnology. Opto-Electron Rev 10:217–224
5. Barnes WL, Dereux A, Ebbesen TW (2003) Surface plasmon subwavelength optics. Nature 424:824–830
6. Qiu J, Shirai M, Nakaya T, Si J, Jiang X, Zhu C, Hirao K (2002) Space-selective precipitation of metal nanoparticles inside glasses. Appl Phys Lett 81:3040–3042
7. Goesmann H, Feldmann C (2010) Nanoparticulate functional materials. Angew Chem Int Ed 49:1362–1395
8. Khlebtsov NG, Dykman LA (2010) Optical properties and biomedical applications of plasmonic nanoparticles. J Quant Spectrosc Radiat Transfer 111:1–35
9. Kreibig U, Vollmer M (1995) Optical properties of metal clusters. Springer, Berlin
10. Puche-Roig A, Martin V, Murcia-Muscarós S, Puchades R (2008) Float glass colouring by ion exchange. J Cult Herit 9:129–133
11. Mazzoldi P, Sada C (2008) A trip in the history and evolution of ion-exchange process. Mater Sci Eng B 149:112–117
12. Vostokov AV, Verzin IA, Ignat'ev AI, Podsvirov OA, Sidorov AI (2010) Comparison of the formation kinetics of silver nanoparticles of photo-thermo-refractive glass after ultraviolet and electron irradiation. Opt Spectrosc 109: 366–371
13. Yang X, Li W, Li Z, Wei Y, Huang W (2008) Depth profiles of Ag nanoparticles in silicate glass. Appl Phys A 90:465–467
14. Blondeau JPh, Catan F, Andreazza-Vignolle C, Sbai N (2008) Plasmon resonance and clustering of silver nanoclusters embedded in glass. Plasmonics 3:65–71
15. Trave E, Gonella F, Calvelli P, Cattaruzza E, Canton P, Cristofori D, Quaranta A, Pellegrini G (2010) Laser beam irradiation of silver doped silicate glasses. Nucl Instrum Methods Phys Res B 268:3177–3182
16. Stepanov AL, Valeev VF, Nuzhidin VI, Bazarov VV, Faizrakhamov IA (2009) Excimer laser-assisted annealing of silicate glass with ion-synthesized silver nanoparticles. Tech Phys 54:1504–1510
17. Varma RS, Kothari DC, Tewari R (2009) Nano-composite soda lime silicate glass prepared using silver ion exchange. J Non-Cryst Solids 355:1246–1251
18. Nacharov AP, Nikonorov NV, Jiang X, Sidorov AI, Tsekhomskii VA (2008) Influence of ultraviolet irradiation and heat treatment on the morphology of silver nanoparticles in photothermorefractive glasses. Glass Phys Chem 34:693–699
19. Battie Y, Destouches N, Bois L, Chassagneux F, Tishchenko A, Parola S, Boukenter A (2010) Growth mechanisms and kinetics of photoinduced silver nanoparticles in mesostructured hybrid silica films under UV and visible illumination. J Phys Chem C 114:8679–8687
20. Zhang J, Dong W, Sheng J, Zheng J, Li J, Qiao L, Jiang L (2008) Silver nanoclusters formation in ion-exchanged glasses by thermal annealing, UV-laser and X-ray irradiation. J Cryst Growth 310:234–239
21. Zeng H, Zhao C, Qiu J, Yang Y, Chen G (2007) Preparation and optical properties of silver nanoparticles induced by a femtosecond laser irradiation. J Cryst Growth 300:519–522
22. Kadono K, Itakura N, Akai T, Yamashita M, Yazawa T (2010) Formation of color centers in a soda-lime silicate glass by excimer laser irradiation. J Phys Condens Matter 22:045901 (7 pp)
23. Zeng H, Qiu J, Jiang X, Qu S, Zhu C, Gan F (2003) Influence of femtosecond laser irradiation and heat treatment on precipitation of silver nanoparticles in glass. Chin Phys Lett 20:932–934
24. Zeng H, Qiu J, Jiang X, Zhu C, Gan F (2004) The effect of femtosecond laser irradiation conditions on precipitation of silver nanoparticles in silicate glasses. J Phys Condens Matter 16:2901–2906
25. Kanehira S, Miura K, Hirao K (2008) Ion exchange in glass using femtosecond laser irradiation. J Cryst Growth 93:023112 (3 pp)
26. Blondeau J-P, Pellerin S, Vial V, Dzierżęga K, Pellerin N, Andreazza-Vignolle C (2008) Influence of pulsed laser irradiation on precipitation of silver nanoparticles in glass. J Cryst Growth 311:172–184
27. De Marchi G, Mattei G, Mazzoldi P, Sada C (2002) Two stages in the kinetics of gold cluster growth in ion-implanted silica during isothermal annealing in oxidizing atmosphere. J Appl Phys 92:4249–4254
28. Hövel H, Fritz S, Hilger A, Kreibig U, Vollmer M (1993) Width of cluster plasmon resonances: bulk dielectric functions and chemical interface dumping. Phys Rev B 48:18178–18188
29. Véron O, Blondeau J-P, Abdelkrim N, Ntsoenzok E (2010) Structural changes of $Ag^+$–$Na^+$ annealed ion-exchanged silicate glasses scanning electron microscopy, far-infrared reflectivity, UV–visible absorption, and TEM investigation. Plasmonics 5:213–219
30. Shaaban MH, Mahmoud KR, Sharshar T, Ahmed AA (2007) Positron annihilation lifetime study of Ag-ion exchanged and heat treated soda lime glass. Nucl Instrum Methods Phys Res B 258:352–356
31. Stalmashonak A, Podlipensky A, Seifert G, Graener H (2009) Transformation of silver nanospheres embedded in glass to nanodisks using circularly polarized femtosecond pulses. Appl Phys B 94:459–465
32. Cabalin LM, Laserna JJ (1998) Experimental determination of laser induced breakdown thresholds of metals under nanosecond Q-switched laser operation. Spectrochim Acta Part B 53:723–730
33. Nagayama K, Kotsuka Y, Kajiwara T, Nishiyama T, Kubota S, Nakahara M (2007) Pulse laser ablation of ground glass. Shock Waves 17:171–183